11th International Conference on Vibration Problems
Z. Dimitrovová *et al.* (eds.)
Lisbon, Portugal, 9-12 September 2013

GBT-BASED VIBRATION ANALYSIS OF THIN-WALLED STEEL FRAMES

Cilmar D. Basaglia[1], **Dinar R.Z. Camotim***[2], **Humberto B. Coda**[1]

[1] Structural Engineering Department, São Carlos School of Engineering, University of São Paulo, Brazil
cbasaglia@usp.br, hbcoda@sc.usp.br

[2]Instituto Superior Técnico, Technical University of Lisbon, Lisbon, Portugal
dcamotim@civil.ist.utl.pt

Keywords: Thin-Walled Steel Frames, Generalised Beam Theory (GBT), Vibration of Loaded Frames, Local Vibration, Global Vibration.

Abstract. *This paper reports the results of an ongoing investigation on the use of Generalised Beam Theory (GBT) to analyse the vibration behaviour of thin-walled steel frames. After a brief overview of the main concepts and procedures involved in performing a GBT vibration analysis, the formulation and implementation of a GBT-based beam finite element are presented, namely the determination of the finite element and frame linear and geometric stiffness matrices, as well as the frame mass matrix (incorporating the influence of the loading and frame joint configurations). Finally, in order to illustrate the application and capabilities of the proposed GBT-based finite element formulation, numerical results concerning the local, distortional and global vibration behaviour of a symmetric portal frame are presented and discussed. For validation purposes, most GBT-based results are compared with values obtained by means of shell finite element analyses carried out in the code ANSYS.*

1 INTRODUCTION

The thin-walled steel frames commonly used in the construction industry are often formed by members (columns, beams or beam-columns) with rather slender open cross-sections, which invariably exhibit very low torsion stiffness and a strong susceptibility to local, distortional and/or global buckling phenomena. Furthermore, given the strong mathematical similarity between the buckling and vibration analysis of structures (similar eigenvalue problems), it is just logical to expect the vibration behaviour of thin-walled frames to be also highly influenced by (i) the member cross-section (local and distortional) deformation (*e.g.*, [1]), (ii) the localised displacement restraints, due to bracing systems (*e.g.*, [2]) and (iii) the frame joint behavioural features (*e.g.*, [3]).

Since most thin-walled steel frames are subjected to *simultaneous* static and dynamic actions (*e.g.*, the effects of heavy machinery or seismic activity), designers are faced with the need of assessing their dynamic response. Therefore, they must be equipped with numerical tools to determine the local and global frame vibration behaviour, eventually in the presence of more or less significant internal forces or moments. However, this task can only be rigorously performed currently by resorting to shell finite element analysis, a highly computer-intensive approach that (i) requires a large modelling effort (including data input and result interpretation) and, therefore, (ii) is still prohibitive for routine applications (*e.g.*, [4]).

One very promising alternative to the above approach is the use of a one-dimensional model based on Generalised Beam Theory (GBT) – a beam theory incorporating genuine folded-plate concepts. In this context, the authors have been employing GBT-based beam finite element formulations to study the buckling behaviour of frames (*e.g.*, [5]) – however, up until now all GBT vibration formulations dealt exclusively with isolated structural members (*e.g.*, [6,7]).

The aim of this paper is to propose and validate an extension of the above GBT-based beam finite element formulations that make it possible to perform local, distortional and global vibration analyses of thin-walled steel frames. In particular, the determination of the finite element and frame linear and geometric stiffness matrices, as well as the frame mass matrix, is addressed. In order to illustrate the application and capabilities of the proposed GBT-based approach, the vibration behaviour of a load-free symmetric portal frame is first analysed. Then, since it is common practice in literature to express the static loading as a fraction of its critical buckling value, the frame buckling behaviour is studied. Finally, the vibration behaviour of the loaded frame is investigated, focusing mainly on the effect of the load magnitude on the fundamental frequency value and mode shape nature. For validation purposes, some GBT results are compared with numerical values obtained by means of shell finite element analyses performed in the commercial code ANSYS [8].

2. GBT VIBRATION ANALYSIS

Because the cross-section displacement field is expressed as a linear combination of mechanically meaningful deformation modes, GBT analyses involve solving equilibrium equations written in a very convenient modal form, thus leading to solution that provide a very clear insight on the member structural response. The performance of a vibration analysis involves (i) a cross-section analysis, to obtain the deformation modes and corresponding mechanical properties, and (ii) the frame analysis, *i.e.*, the solution of the vibration eigenvalue problem and the (modal) interpretation of the results determined (natural frequencies and mode shapes).

Consider the arbitrary thin-walled open-section member shown in Fig. 1(a). In each wall, one defines a local coordinate system *x*-*s*-*z*, as depicted in Fig. 1(b) – *u*, *v* and *w* are the associated displacement components (*x* is the longitudinal direction and *u* are warping displacements).

The GBT displacement field representation adopts the classical beam theory variable separation

$$u(x,s,t) = u_k(s)\zeta_{k,x}(x,t) \qquad v(x,s,t) = v_k(s)\zeta_k(x,t) \qquad w(x,s,t) = w_k(s)\zeta_k(x,t) \qquad (1)$$

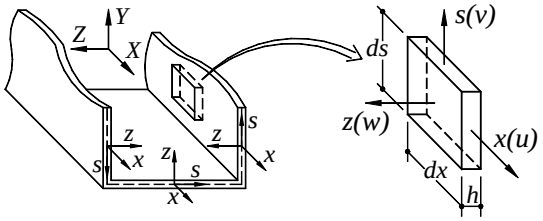

Figure 1: Arbitrary thin-walled open cross-section, coordinate axes and displacements.

where (i) x and s are coordinates along the member axis and cross-section midline, (ii) functions $u_k(s)$, $v_k(s)$ and $w_k(s)$, yielded by the cross-section analysis (*e.g.*, [9]), provide the longitudinal, transverse membrane and transverse flexural displacements of deformation mode k, (iii) $(.)_{,x} \equiv d(.)/dx$, (iv) the summation convention applies to subscript k and (v) $\zeta_k(x,t)$ are the functions describing the variation of the deformation mode amplitudes both along the longitudinal direction and with time t.

Fig. 2 shows the dimensions and a possible GBT discretisation of the lipped channel cross-sections dealt with in this work – all frame members have elastic constants $E=205$ *GPa* (Young's modulus) and $\upsilon=0.3$ (Poisson's ratio). The cross-section analysis yields *17* deformation modes – the in-plane shapes of the *9* most relevant ones, *i.e.*, those contributing to the sought frame vibration modes, are also shown in Fig. 2.

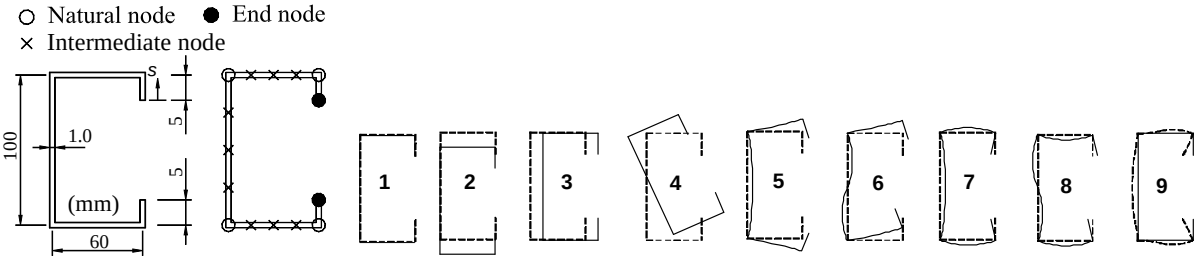

Figure 2: Lipped channel section: geometry, GBT discretisation and in-plane shape of the *9* most relevant deformation modes.

After determining the deformation modes, the equilibrium equation system defining the dynamic problem can be readily established,

$$C_{ik}\zeta_{k,xxxx} - D_{ik}\zeta_{k,xx} + B_{ik}\zeta_k - Q_{ik}\zeta_{k,xxtt} + R_{ik}\zeta_{k,tt} - X_{jik}\left(W_j^0\zeta_{k,x}\right)_{,x} = 0 \qquad (2)$$

where, C_{ik} (warping displacement), D_{ik} (torsional rotations) and B_{ik} (local deformations) are cross-section modal mechanical properties, (iii) X_{jik} are geometric stiffness components associated with normal stress resultants W_j^0 due to uniform compression ($j=1$) and/or bending ($j=2,3$), and (iv) R_{ik} and Q_{ik} are mass components that account for the influence of the inertia forces on the out-of-plane and in-plane cross-section displacements, and are given by

$$C_{ik} = E\int_S \left[hu_i u_k + \frac{h^3}{12(1-\nu^2)} w_i w_k \right] ds \qquad B_{ik} = \frac{E\,h^3}{12(1-\nu^2)} \int_S w_{i,ss}\, w_{k,ss}\, ds$$

$$D_{ik} = \frac{Gh^3}{3}\int_S \left[w_{i,s}\, w_{k,s} - \frac{\nu}{2(1-\nu)}\left(w_i\, w_{k,ss} + w_k\, w_{i,ss}\right) \right] ds \qquad (3)$$

$$X_{jik} = \frac{E\,h}{C_{jj}} \int_S u_j (v_i v_k + w_i w_k) ds \tag{4}$$

$$Q_{ik} = \rho h \int_S u_i u_k ds + \frac{\rho h^3}{12} \int_S w_i w_k ds \qquad R_{ik} = \rho h \int_S (v_i v_k + w_i w_k) ds + \frac{\rho h^3}{12} \int_S w_{i,s} w_{k,s} ds \tag{5}$$

where (i) h is the wall thickness (uniform) and (ii) ρ is the material mass density (deemed uniform and equal to $7.85g/cm^3$ in this work).

One solution of system (2) can be found by assuming that the free vibration motions are synchronous, *i.e.*, by adopting the separation of variables

$$\zeta_k(x,t) = \phi_k(x) Y(t) \tag{6}$$

where $\phi_k(x)$ is a longitudinal shape function and $Y(t)$ is a time-dependent function satisfying the free vibration harmonic equation of motion $Y_{,tt} + \omega^2 Y = 0$, where ω is the angular frequency of vibration – thus, one may write

$$\zeta_{k,tt} = -\omega^2 \zeta_k \tag{7}$$

The insertion of (7) into (2) leads to the final system of equilibrium equations

$$C_{ik}\phi_{k,xxxx} - D_{ik}\phi_{k,xx} + B_{ik}\phi_k - \omega^2 \left(R_{ik}\phi_k - Q_{ik}\phi_{k,xx}\right) - X_{jik}\left(W_j^0 \phi_{k,x}\right)_{,x} = 0 \tag{8}$$

which depends exclusively on derivatives with respect to x.

2.1 Frame Analysis

In isolated members, the solution of (8) is obtained by means of a beam finite element formulation developed and implemented by Bebiano *et al.* [7]: 2-node elements with $2n$ degrees of freedom per node (n is the number of deformation modes included in the analysis) and using Hermite cubic polynomials $\psi_i(x)$ to approximate the mode amplitude functions $\phi_k(x)$ – one then has

$$\phi_k(x) = \psi_1(\xi)\, d_{k1} + \psi_2(\xi)\, d_{k2} + \psi_3(\xi)\, d_{k3} + \psi_4(\xi)\, d_{k4} \tag{9}$$

where $d_{k1} = \phi_{k,x}(0)$, $d_{k2} = \phi_k(0)$, $d_{k3} = \phi_{k,x}(L_e)$, $d_{k4} = \phi_k(L_e)$, $\xi = x/L_e$ (L_e is the element length) and

$$\psi_1(\xi) = L_e(\xi^3 - 2\xi^2 + \xi) \quad \psi_2(\xi) = 2\xi^3 - 3\xi^2 + 1 \quad \psi_3(\xi) = L_e(\xi^3 - \xi^2) \quad \psi_4(\xi) = 3\xi^2 - 2\xi^3 \tag{10}$$

Thus, the various sub-matrix components of the finite element linear stiffness $[K_e]$ and mass $[M_e]$ matrices are determined by means of the expressions

$$K_{ik}^{pr} = C_{ik} \int_{L_e} \psi_{p,xx} \psi_{r,xx} dx + D_{ik} \int_{L_e} \psi_{p,x} \psi_{r,x} dx + B_{ij} \int_{L_e} \psi_p \psi_r dx$$

$$M_{ik}^{pr} = Q_{ik} \int_{L_e} \psi_{p,x} \psi_{r,x} dx + R_{ik} \int_{Le} \psi_p \psi_r dx \tag{11}$$

where (i) subscripts i, $k=1\ldots n$ identify the deformation modes associated with each sub-matrix and (ii) superscripts p, $r=1\ldots 4$ concern the finite element degrees of freedom involved in each sub-matrix.

After discretising the frame, one must handle separately the degrees of freedom concerning the member (i) internal nodes and (ii) end nodes associated with frame joints connecting members with different orientations – see Figs 3(a)-(b). In the former, one always considers GBT modal degrees of freedom (values and derivatives of the discretised amplitude functions $\phi_k(x)$), as the compatibility between them is trivially ensured (*e.g.*, [7]). The same is not true

for the joint nodes (*e.g.*, nodes b_r and a_{r+1} in Fig. 3(b)), where guaranteeing the compatibility between the GBT degrees of freedom of the converging finite element end sections it is not a straightforward matter – this stems from their modal nature and the fact that they are referred to distinct (member) coordinate systems. In order to overcome this difficulty, one must first (i) "transform" these modal degrees of freedom into *nodal* generalised displacements of the point where the joint is assumed to take place (usually the intersection of the member centroidal axes), a task carried out by resorting to a "*joint element*" concept, and (ii) impose constraint conditions to model the compatibility between the end section displacements caused by distortional warping and wall transverse bending (see Fig. 3(c)).

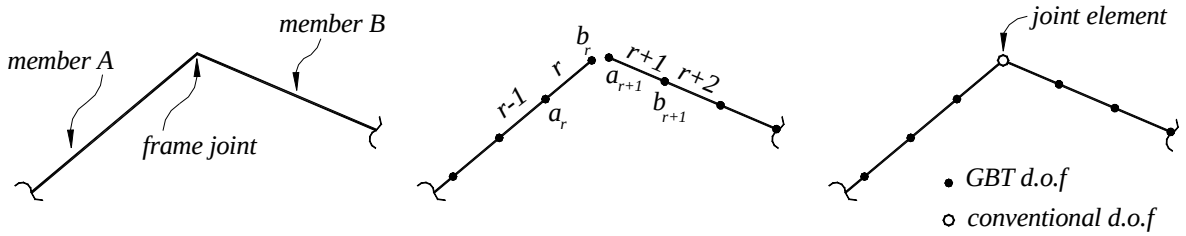

Figure 3: (a) Frame joint, (b) discretisation of the converging members and (c) "joint element" concept.

Next, one addresses the concepts and describes the procedures involved in determining the frame linear and geometric stiffness matrices, as well as the frame mass matrix, on the basis of their GBT-based finite element counterparts:

(i) To ensure displacement compatibility at the "joint element", one uses the transformation matrix $[T]$, relating the GBT (member) and nodal (joint) degrees of freedom and defined by the expressions

$$\{\bar{\xi}\} = [T]\{d\} \Leftrightarrow \begin{Bmatrix} \{\bar{\xi}_G\} \\ \{\bar{\xi}_D\} \\ \{\bar{\xi}_L\} \end{Bmatrix} = \begin{bmatrix} [R_{\bar{Y}+\bar{Z}}][R_X][L]_{6x6} & \\ & [I]_{qxq} \end{bmatrix} \begin{Bmatrix} \{d_G\} \\ \{d_D\} \\ \{d_L\} \end{Bmatrix} \tag{12}$$

$$\{\bar{\xi}_G\} = \{U_{\bar{X}} \;\; U_{\bar{Y}} \;\; U_{\bar{Z}} \;\; \Theta_{\bar{X}} \;\; \Theta_{\bar{Y}} \;\; \Theta_{\bar{Z}} \;\; \Theta'_{\bar{X}}\}^T \qquad \{d_G\} = \{u \;\; v_Y \;\; v_Z \;\; \varphi_X \;\; \theta_Y \;\; \theta_Z \;\; \varphi'\}^T$$

$$\{\bar{\xi}_D\} = \{\bar{\mu}'_{k=5} \;\; \bar{\mu}_{k=5} \;\; \ldots \;\; \bar{\mu}'_{k=5+n_d-1} \;\; \bar{\mu}_{k=5+n_d-1}\}^T \qquad \{d_D\} = \{\mu'_{k=5} \;\; \mu_{k=5} \;\; \ldots \;\; \mu'_{k=5+n_d-1} \;\; \mu_{k=5+n_d-1}\}^T$$

$$\{\bar{\xi}_L\} = \{\bar{\beta}'_{k=5+n_d} \;\; \bar{\beta}_{k=n} \;\; \ldots \;\; \bar{\beta}'_{k=5+n_d} \;\; \bar{\beta}_{k=n}\}^T \qquad \{d_L\} = \{\beta'_{k=5+n_d} \;\; \beta_{k=n} \;\; \ldots \;\; \beta'_{k=5+n_d} \;\; \beta_{k=n}\}^T$$

where (i_1) $\{\bar{\xi}_G\}$ is the global mode nodal generalised displacement sub-vector (referred to axes $\bar{X}-\bar{Y}-\bar{Z}$ – see Fig. 4(a)), (i_2) the sub-vector $\{\bar{\xi}_L\}$ and $\{\bar{\xi}_D\}$ components concern the local and distortional generalised displacements, (i_3) $\{d_G\}$, $\{d_D\}$ and $\{d_L\}$ contain the GBT degrees of freedom, (i_4) matrix $[R_{\bar{Y}+\bar{Z}}]$ describes the transformation associated with successive rotations about axes $\bar{Z}$ (firstly) and $\bar{Y}$ (secondly), defined by matrices $[R_{\bar{Z}}]$ and $[R_{\bar{Y}}]$, (i_5) matrix $[R_X]$ provides the rotation about the member axis X (see Fig. 4(b)), (i_6) $[I]$ is an identity matrix associated with the torsion warping, local and distortional displacements, with maximum dimension $q=2c+1$ (c is the number of local and distortional modes included in the analysis) and (i_7) $[L]$ is a translation matrix relating the connected element/member generalised displacements (originally referred to centroidal G or shear centre S longitudinal axes) to parallel reference axes passing through point $\bar{O}$, where the joint is deemed "materialised" (see Fig. 4(b)). The components of matrices $[R_{\bar{Y}+\bar{Z}}]$, $[R_X]$ and $[L]$ are given in Basaglia *et al.* [10].

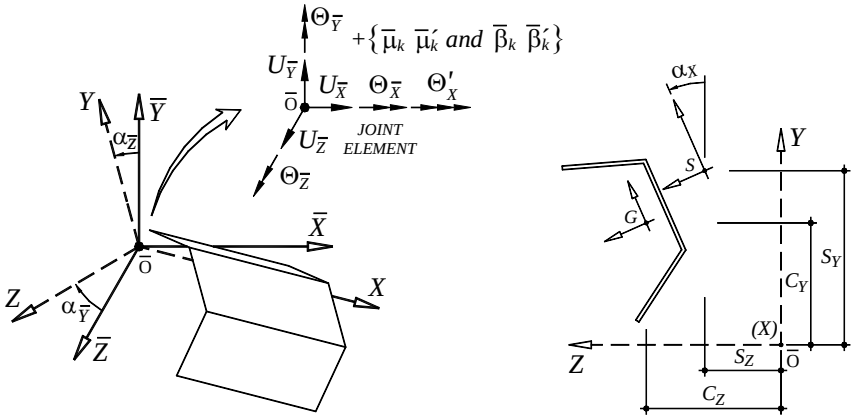

Figure 4: (a) "Joint element" and member (global) coordinate systems, and (b) cross-section (local) coordinate system and relative positions of points *G*, *S* and $\overline{O}$.

(ii) By using the transformation matrix given in (12), one defines, in each joint member end section, (ii_1) *7* global mode degrees of freedom and (ii_2) $q-1$ degrees of freedom associated with local and distortional modes – they must satisfy the conditions

$$\{\overline{\xi}\}_{b_r} = \begin{bmatrix} [W]_{7\times 7} & \\ & \Pi \end{bmatrix} \{\overline{\xi}\}_{a_{r+1}} \tag{13}$$

where (ii_1) subscripts *b* and *a* identify the end sections of the connected members *r* and *r+1* (see Fig. 3(b)), (ii_2) Π are "*constraint conditions*" that ensure the compatibility between the wall warping and flexural displacements and (ii_3) [*W*] is a diagonal matrix whose components W_{ii} relate the generalised global displacements and rotations of each end cross-section.

(iii) Depending on the particular joint configuration, the relations between the connected end section displacements, incorporated into the analysis through the diagonal matrix [*W*], may be either *complete* or *incomplete*. These two cases correspond to non-null components $|W_{ii}|=1$ or $|W_{ii}|\neq 1$, which are associated with the (iii_1) rotations due to bending and torsion (W_{44} and W_{55}) and (iii_2) torsion warping displacement (W_{77}) – their values were already presented in detail in [10,11].

(iv) The *constraint conditions* Π (iv_1) vary with the member cross-section shape and the joint configuration, and (iv_2) involve the displacements in *i* natural and *j* intermediate nodes of the connected end sections – these conditions can be expressed in the form

$$\Pi_{i,j} = \{\Delta\}^T \{\phi_k\} = 0 \tag{14}$$

where the vector $\{\Delta\}$ components are either (iv_1) warping functions $u_k(s)$ or (iv_2) wall flexural functions $w_k(s)$. The particular "constraint conditions" considered in this work is addressed in [11].

(v) Once all the member support and joint compatibility conditions are enforced, the frame linear $[\widetilde{K}]$ and geometric $[\widetilde{G}]$ stiffness matrices and mass matrix $[\widetilde{M}]$ are readily obtained, which are expressed in terms of "mixed" degrees of freedom: GBT modal and "conventional" nodal ones. The joint compatibility is incorporated into the stiffness matrix by means of the matrix operation

$$([\widetilde{K}] - [\widetilde{G}] - \omega^2[\widetilde{M}]) = [\Omega]^T ([K] - [G] - \omega^2[M])\,[\Omega] \tag{15}$$

where (v_1) the tilde (~) identifies the matrices associated with joint compatibility conditions and (v_2) the compatibility matrix $[\Omega]$,

$$\{d\} = [\Omega]\{\tilde{d}\} \tag{16}$$

contains the joint modal displacement values (*i.e.*, $u_k(s)$, $v_k(s)$ or $w_k(s)$) – $\{\tilde{d}\}$ is a "mixed" vector combining generalised displacements and GBT degrees of freedom.

After determining the frame total stiffness and mass matrices ($[\tilde{K}]-[\tilde{G}]-\omega^2[\tilde{M}]$), one (i) solves the vibration eigenvalue problem and (ii) transforms the nodal degrees of freedom (joint generalised displacements) back into GBT ones, through the operation defined in (16) – this last procedure makes it possible to obtain a fully modal representation of the frame vibration modes (*i.e.*, identify and quantify the individual contributions of the deformation modes of the various members), a feature that provides a decisive contribution towards a more in-depth understanding of the mechanical aspects involved in the local, distortional and global vibration behaviour of thin-walled frames.

3. ILLUSTRATIVE EXAMPLES

In order to validate and illustrate the application and potential of the proposed GBT-based beam finite element approach, numerical results are presented and discussed next. They concern the local, distortional and global vibration of the symmetric portal frame depicted in Fig. 5(a), which is formed by three lipped channel members (*A*, *B*, *C*) (i) with identical cross-sections (dimensions given in Fig. 2) and (ii) made of steel ($E=205\,GPa$ and $\nu=0.3$). The frame has fixed column bases and joints with flange continuity. One begins by analysing the vibration behaviour of the load-free frame. Then, the buckling behaviour of the frame subjected only to uniform axial compression diagrams ($N_A=N_C=0.83P$ and $N_B=1.0P$ – see Fig. 5(b)) is analysed. Finally, the vibration behaviour of the loaded frame is investigated – the static applied loading is always expressed as a percentage of the associated critical buckling load (P_{cr}). For validation, most GBT-based results are compared with values yielded by ANSYS [8] shell finite element analyses.

The GBT analyses are based on frame discretisations into *52* finite elements, which correspond to *106* degrees of freedom for each deformation mode included in the analysis. Thus, an analysis including all *17* deformation modes stemming from the adopted GBT discretisation (see Fig. 2) involves *1590 d.o.f.*. On the other hand, the ANSYS shell finite element analyses involve more than *16000 d.o.f.*.

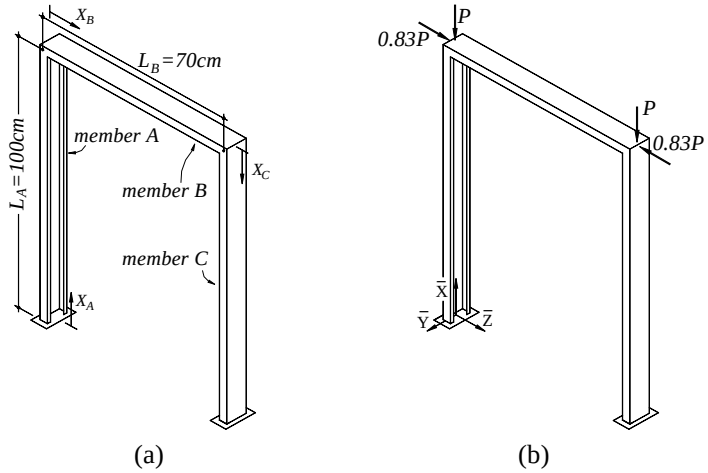

Figure 5: Symmetric portal frame: (a) geometry and (b) loading.

3.1 Load-free Frame Vibration

Table 1 shows the first eight natural frequencies (in rad/s), obtained by means of the GBT analysis (ω_{GBT}) and shell finite element analysis (ω_{ANSYS}). Fig. 6 provides, for each of the three frame members, the amplitude functions $\phi_k(x)$ of the deformation modes that participate in the first four frame vibration modes. As for Fig. 7, it displays the configurations of theses vibration modes obtained from the ANSYS shell finite element analysis. The observation and comparison between

Table 1. GBT and ANSYS frame vibration frequencies (rad/s).

Vibration mode	ω_{GBT}	ω_{ANSYS}	Δ (%)
1	392.72	383.54	2.4
2	451.81	446.10	1.3
3	630.90	630.27	0.1
4	653.80	635.17	2.9
5	665.04	645.35	3.1
6	685.12	670.04	2.3
7	779.01	763.66	2.0
8	785.05	768.12	2.2

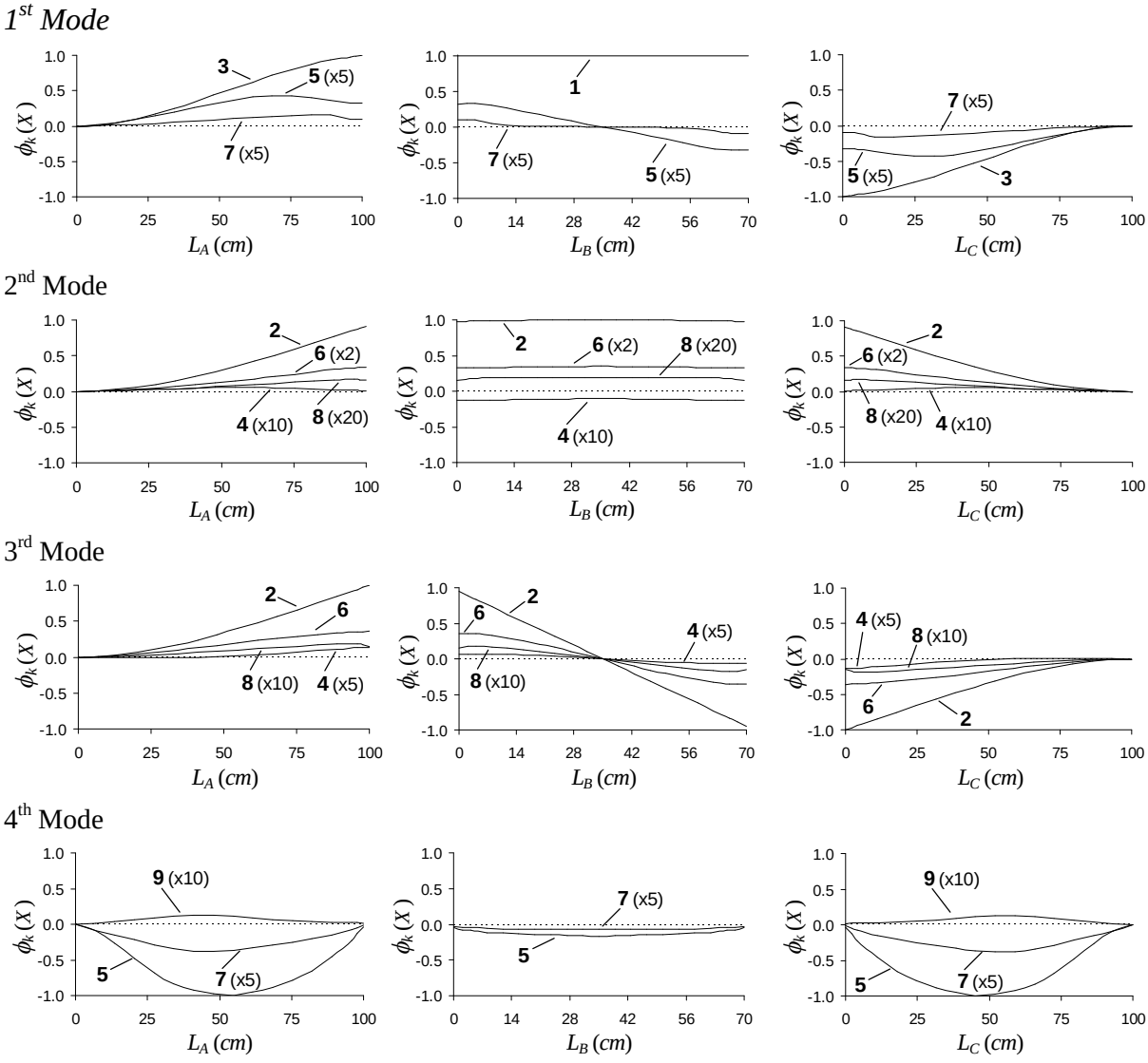

Figure 6: Modal amplitude function $\phi_k(x)$ that participate in the first four frame vibration modes.

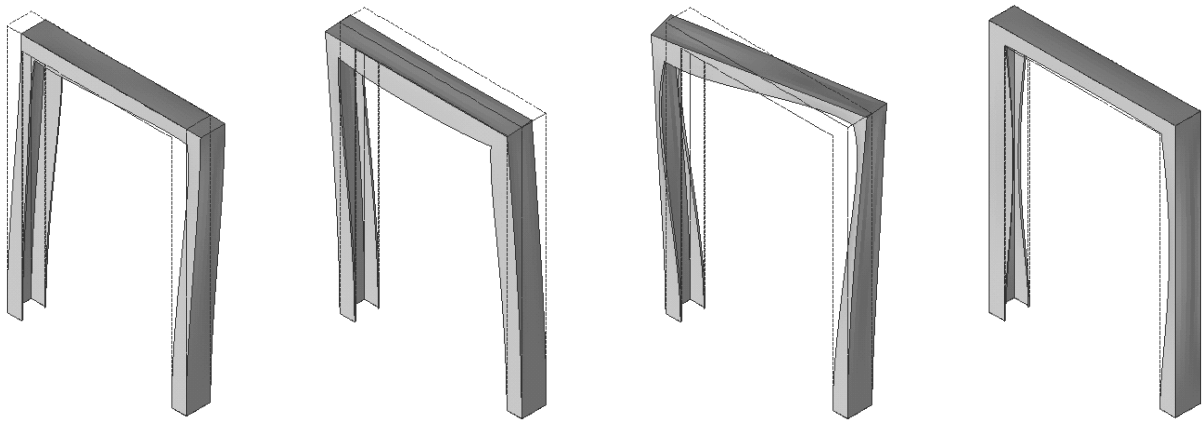

Figure 7: First four frame vibration modes obtained by ANSYS.

the vibration results yielded by the two numerical models prompts the following main remarks:

(i) The natural frequencies yielded by the GBT-based and ANSYS shell finite element analyses practically coincide – the maximum difference is *3.1%*.

(ii) There is also a very close agreement between the GBT modal amplitude functions and the vibration mode shapes obtained from the ANSYS analysis. However, it can be easily argued that the GBT representation enables a better quantitative and qualitative insight on this frame vibration behaviour.

(iii) The local and distortional deformation modes become more relevant as the vibration mode order increase. Indeed, wile the global modes **2** and **3** are predominant in the first three vibration modes, in the fourth vibration mode prevail modes **5** and **7**.

3.2 Frame Buckling

Fig. 8 provides two representations of critical buckling mode shapes of the frame considered in this work, namely (i) GBT modal amplitude functions and (ii) ANSYS 3D views. The observation of these two sets of buckling results prompts the following remarks:

(i) The GBT and ANSYS critical loads are very similar – one has $P_{cr.GBT}=19.25kN$ and $P_{cr.ANSYS}=18.72kN$ (differences below *2.83 %*).

(ii) The frame buckles in a combination of local and distortional deformation modes that (ii_1) involves the three members and (ii_2) includes contributions from the GBT deformation modes **5**

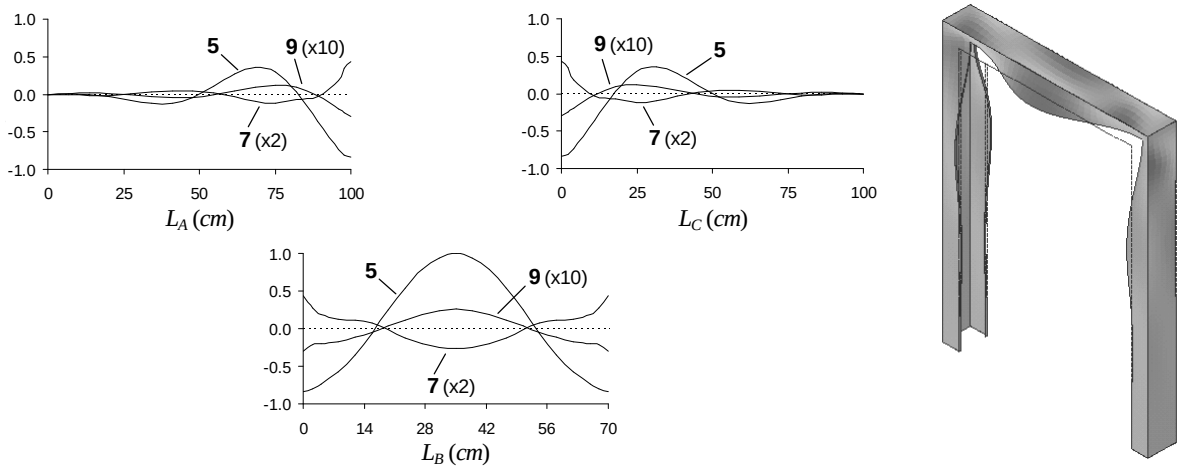

Figure 8: Frame critical buckling mode: modal amplitude functions (GBT) and three-dimensional configuration (ANSYS).

(distortional) and **7**+**9** (local). The participation of mode **5** is highly dominant (*75%*), with the maximum values occurring at the member *B* mid-span region, but there are also non-negligible contributions from local modes **7** and **9** in the joint vicinities.

3.3 Loaded Frame Vibration

Finally, one investigates the vibration of frames subjected to uniform axial compression loads – the applied load value is defined by a parameter $P^0 \equiv W_1^0$, which is taken as fraction (α) of its critical value, *i.e.*, $P^0 = \alpha P_{cr}$. Table 2 shows the influence of the applied loading (α=*0, 0.25, 0.5, 0.75, 0.95, 0.99*) on the frame fundamental frequency ω_1. Moreover, the 3D views yielded by ANSYS and the modal amplitude functions presented in Fig. 9 and 10 (three load levels) provide in-depth information on the evolution of the frame fundamental vibration mode as the applied load level increases. After observing the results presented in these figures and table, the following conclusions can be drawn:

(i) The presence of loading only cause a considerable fundamental frequency drop (*i.e.*, more than *5%*) for $\alpha \geq 0.75$ – a substantial fundamental frequency drop (*i.e.*, more than *30%*) occur for $\alpha \geq 0.95$.

(ii) The GBT and ANSYS fundamental frequencies are again extremely close (differences below *3.4%*). Moreover, there is also excellent correlation between the fundamental vibration mode shapes provided by the ANSYS analyses and GBT modal amplitude functions.

(iii) The comparison between the modal amplitude functions for α=*0* (see Fig. 10) and $\alpha \neq 0$, shows that the fundamental vibration mode shapes of the load-free frame and the loaded frame with α=*0.25* are very similar. On the other hand, the fundamental vibration mode shape is considerably altered by the presence of a load level equal to α=*0.75* – indeed, there is an increase of the contribution of the deformation modes **5** and **7**.

(iv) For $\alpha \cong 1$ the vibration mode shape changes quite drastically, approaching its critical buckling mode counterpart – indeed, for α=*0.99* the fundamental vibration and critical buckling modes virtually coincide, as attested by the comparison with Fig. 8.

Table 2: Variation of the fundamental frequencies (rad/s) with α

α	ω_{GBT}	ω_{ANSYS}	Δ (%)
0	392.72	383.54	2.4
0.25	387.69	377.58	2.7
0.50	382.31	370.44	3.2
0.75	370.13	358.32	3.3
0.95	269.21	261.43	3.0
0.99	133.94	130.30	2.8

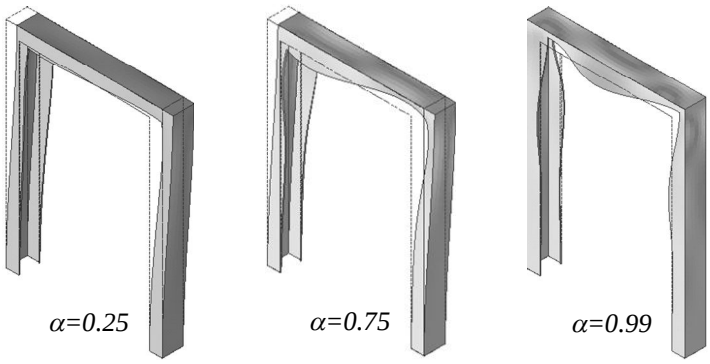

Figure 9: Fundamental vibration modes for α=*0.25, 0.75, 0.99.*

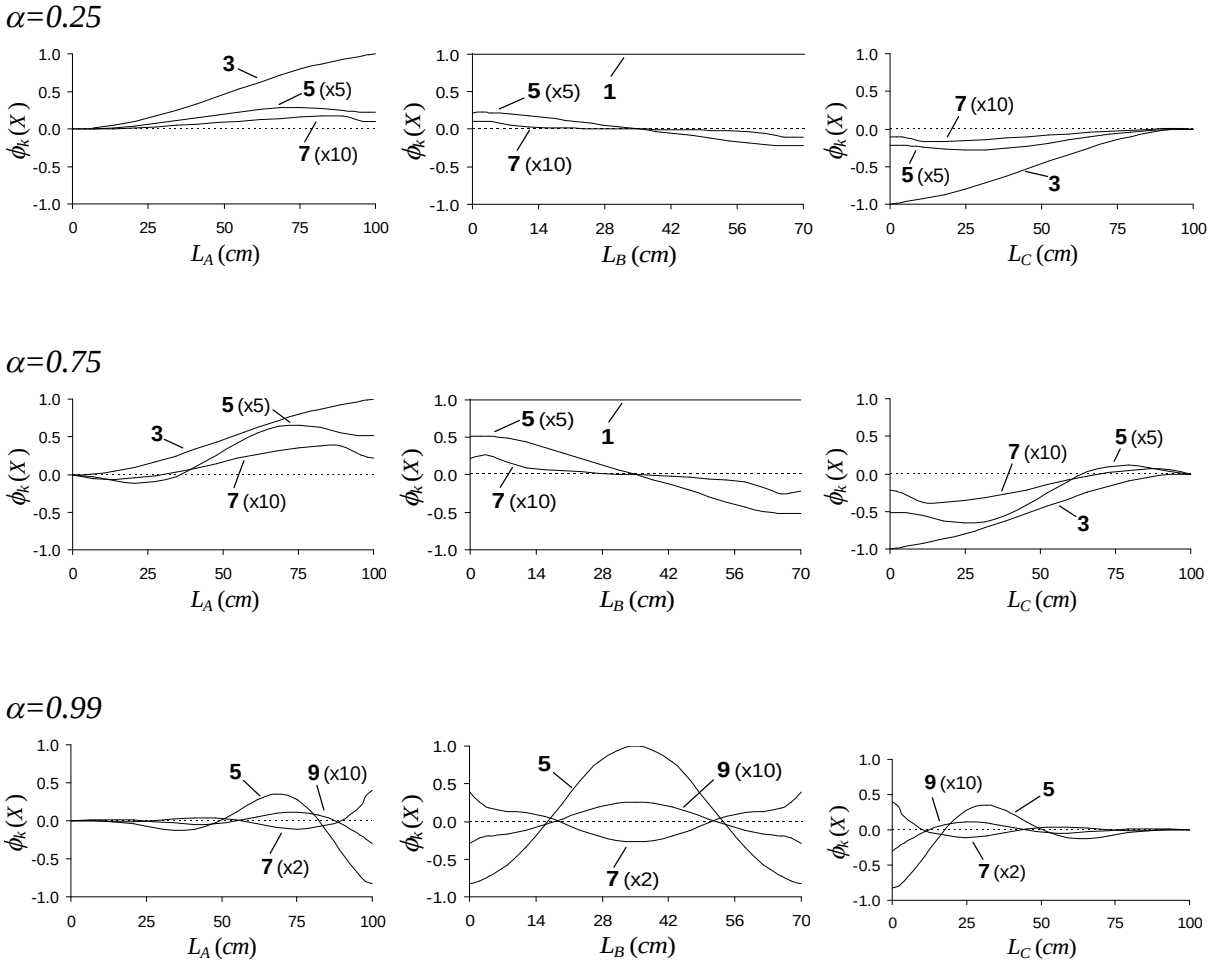

Figure 10: Modal amplitude functions $\phi_k(X)$ that participate in the fundamental vibration modes for α=*0.25*, *0.75*, *0.99*.

4. CONCLUSION

The paper reported the results of an ongoing investigation on the use of a GBT-based beam finite element approach to analyse the local, distortional and global vibration behaviour of thin-walled steel frames. After a very brief review of the most relevant concepts involved in performing a GBT vibration analysis, the paper described the procedures involved in obtaining the frame overall linear and geometric stiffness matrices, as well as the frame mass matrix, which incorporate the effect of the frame joints. Finally, the application and capabilities of the developed GBT-based beam finite element approach were illustrated by means of the presentation and discussion of numerical results concerning the local, distortional and global vibration behaviour of load-free and loaded symmetric portal frames – the study focused on the influence of the applied load level on the vibration frequencies and mode shapes. For validation purposes, most of the GBT-based results were compared with values obtained by means of shell finite element analyses carried out in the code ANSYS. An excellent agreement was found in all cases, despite the large difference between the numbers of *d.o.f.* involved in the two analyses.

ACKNOWLEDGMENTS

The financial support of *Fundação para a Ciência e Tecnologia* (FCT – Portugal), through project PTDC/ECM/108146/2008, and *Fundação de Amparo à Pesquisa do Estado de São Paulo* (FAPESP – Brazil), through project 11/15731-5, is gratefully acknowledged.

REFERENCES

[1] T. Ahmed and S. Shimizu, A study of the seismic effects on a portal frame having a hole at the beam-column connection. *Thin-Walled Structures*, **52**(March), 53-60, 2012.

[2] T. Türker and A. Bayraktar, Experimental and numerical investigation of brace configuration effects on steel structures. *Journal of Construction Steel Research*, **67**(May), 854-865, 2011.

[3] D.S. Sophianopoulos. The effect of joint flexibility on the free elastic vibration characteristics of steel plane frames. *Journal of Construction Steel Research*, **59**(8), 995-1008, 2003.

[4] R. Moazed, W. Szyszkowski and R. Fotouhi, The in-plane behaviour and FE modelling of a T-joint connection of thin-walled square tubes. *Thin-Walled Structures*, **47**(6-7), 816-825, 2009.

[5] D. Camotim, C. Basaglia and N. Silvestre, GBT buckling analysis of thin-walled steel frames: a state-of-the-art report. *Thin-Walled Structures*, **48**(10-11), 726-743, 2010.

[6] N. Silvestre and D. Camotim, Vibration behaviour of axially compressed cold-formed steel members, *Steel & Composite Structures – An international Journal*, **6**(3), 231-236, 2006.

[7] R. Bebiano, N. Silvestre and D. Camotim, Local and global vibration of thin-walled members subjected to compression and non-uniform bending. *Journal of Sound and Vibration*, **315**(3), 509-535, 2008.

[8] Swanson Analysis Systems Inc. *ANSYS Reference Manual*, version 12, 2009.

[9] R. Gonçalves, M. Ritto-Corrêa and D. Camotim, A New Approach to the Calculation of Cross-Section Deformation Modes in the Framework of Generalized Beam Theory, *Computational Mechanics*, **46**(5), 759-781, 2010.

[10] C. Basaglia, D. Camotim and N. Silvestre, Global buckling analysis of plane and space thin-walled frames in the context of GBT, *Thin-Walled Structures*, **46**(1), 79-101, 2008.

[11] C. Basaglia, D. Camotim and N. Silvestre, GBT-based local, distortional and global buckling analysis of thin-walled steel frames. *Thin-Walled Structures*, **47**(11), 1246-1264, 2009.